

# High absorbing CuInS<sub>2</sub> thin films growing by oblique angle incidence deposition in presence of thermal gradient

F. CHAFFAR AKKARI, R. BRINI, M. KANZARI, B. REZIG

*Laboratoire de Photovoltaïque et Matériaux Semi-conducteurs -ENIT BP 37, Le belvédère  
1002-Tunis, Tunisie*

*E-mail: mounir.kanzari@ipeit.rnu.tn*

Published online: 25 August 2005

Oblique angle deposition technique can generate nanostructures and has attracted the interest of many researchers. In this article we use this technique to investigate the physical properties of obliquely evaporated CuInS<sub>2</sub> films deposited onto substrates submitted to a thermal gradient. We show that the correlation between the obliquely angle deposition and the thermal gradient leads to an improvement in the optical properties of the films. Indeed high absorption coefficient ( $10^5$ – $3.10^5$  cm<sup>-1</sup>) in the visible range and near-IR spectral range are reached for the small incident angles. Scanning electron microscopy shows that the films had a microstructure with columns that are progressively inclined as the incident angle was increased. © 2005 Springer Science + Business Media, Inc.

## 1. Introduction

Columnar thin films prepared by oblique-angle-incidence deposition have attracted research attention due to their extraordinary morphologies and structures. Thin films with inclined columns can show interesting electromagnetic properties. Dielectric films with inclined columns can be used for retardation plates [1] and for liquid-crystal alignment [2]. Oblique deposition also affects electrical [3], magnetic [4], photoelectric [5] and thermoelectric [6] properties.

The features of the structures of these films, such as the tilt angle  $\beta$  with respect to the surface normal, and the diameter  $d$  and separation  $l$  of the columns, can be tailored by changing the vapour incident angle  $\theta$  with respect to the surface normal, and therefore changing their physical properties. For example, the magnetic domain structure changes from uniform domains to stripe domains with an increase of the incident angle [7–11]. In general, the column tilt angle  $\beta$  is less than the vapour incident angle  $\theta$ , and follows the empirical tangent rule,  $\tan \beta = (1/2) \tan \theta$  for small  $\theta$  [12, 13], or the cosine rule,  $\beta = \theta - \arcsin(\frac{1-\cos\theta}{2})$  [14].

The present article is devoted to CuInS<sub>2</sub> films. The ternary compound semiconductor CuInS<sub>2</sub> is attractive for solar energy conversion due to its band gap of 1.55 eV, which matches the optimum for conversion of the solar spectrum almost perfectly. The highest conversion efficiency reported up to now for a thin film solid state device is 12.2% [15].

The objective of this work is the investigation of the optical and morphological properties of obliquely

evaporated CuInS<sub>2</sub> films in correlation with a thermal gradient.

## 2. Experimental details

### 2.1. Synthesis of CuInS<sub>2</sub>

Stoichiometric amounts of the elements of 99.999% purity Cu, In, and S were used to prepare the initial ingot of CuInS<sub>2</sub>. The mixture was sealed in vacuum in a quartz tube. In order to avoid explosions due to sulfur vapor pressure, the quartz tube was heated slowly (20°C/h). A complete homogenization could be obtained by keeping the melt at 1000°C for about 48 h. The tube was then cooled at the rate 7°C/h. So the cracking, due to thermal expansion of the melt on solidification, was avoided. X-rays of powder analysis showed that only homogenous CuInS<sub>2</sub> phase was present in the ingot. Crushed powder of this ingot was used as raw material for the thermal evaporation.

### 2.2. Film preparation

CuInS<sub>2</sub> films were prepared by an evaporation of the CuInS<sub>2</sub> powder in a high vacuum system with a base pressure of  $10^{-5}$  Torr. Thermal evaporation sources were used which can be controlled either by the crucible temperature or by the source power. The glass substrates were kept at 250°C during the evaporation process. A schematic drawing of the films deposition system is shown in Fig. 1. Substrate orientation was such that the direction of the incident evaporated flux and the substrate normal formed an angle  $\theta$ . Substrate heating was achieved by the heater system described elsewhere [16]. This system allowed us to insert a

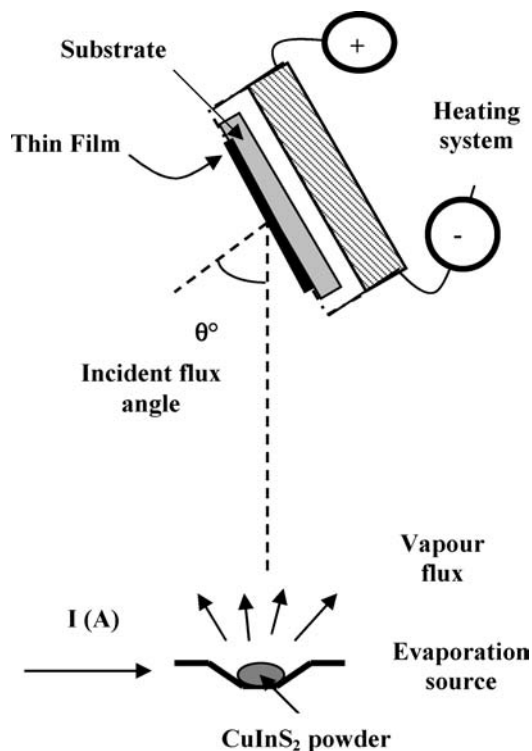


Figure 1 A schematic drawing of the films deposition system.

suitable Cu-based alloy cylinder with a diameter  $d \leq D$ , where  $D$  is the heater diameter ( $D = 100$  mm), between the heater and the substrate holder. The cylinder thickness was kept constant (1 cm). The distance from crucible to sample holder was 10 cm. The substrate temperature was measured using a thermocouple in contact with the substrate surface. Two types of layers are then obtained:

- Samples deposited on homogeneously heated substrates (where conductive heating is dominant,  $d = D$ )
- Samples grown under thermal gradient (where heating by radiation is dominant,  $d = 0$ ).

In this work we correlate the thermal gradient and the substrate orientation to prepare the  $\text{CuInS}_2$  films. For example, we show in Fig. 2 the temperature profile

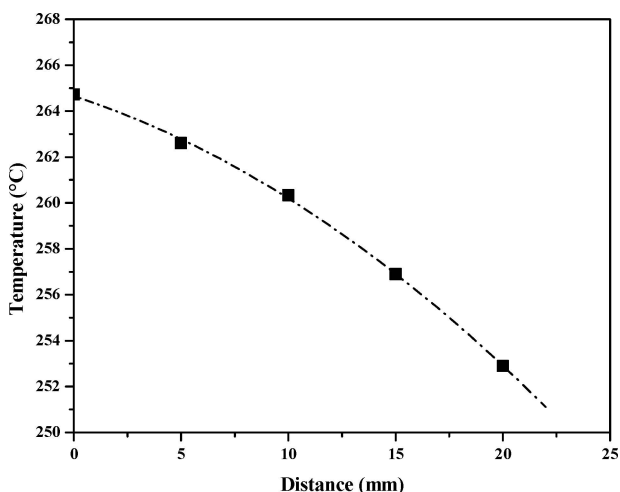


Figure 2 The temperature profile versus the thermocouple position for an incident angle  $\theta = 60^\circ$ .

versus the thermocouple position for an incident angle  $\theta = 60^\circ$ .

## 2.3. Characterization of the $\text{CuInS}_2$ thin films

Optical transmittance ( $T_{\text{exp}}$ ) and reflectance were measured at normal incidence with an UV-visible-NIR Shimadzu 3100S spectrophotometer in the wavelength range 300–1800 nm. The film's thicknesses were calculated from the positions of the interference maxima and minima of reflectance spectra using a standard method [17]. Scanning electron microscopy (SEM) micrographs were performed using a Philips XL30 microscope. The structural properties were determined by the X-ray diffraction technique using  $\text{CuK}_{\alpha 1}$  radiation ( $\lambda = 0.15418$  nm).

## 3. Results and discussion

### 3.1. Structural properties

Figs 3a–e show the results of our XRD measurements for different oblique angles. It was found that the oblique angle had great effects on the growth of polycrystalline  $\text{CuInS}_2$  films in particular for the higher oblique angles. Indeed, All diagrams present a peak ( $2\theta \approx 27.90^\circ$ ) which we have assigned to the (112) reflection of  $\text{CuInS}_2$  phase at an angle of incidence below  $75^\circ$  the films showed additional peaks that can be associated to binary compounds ( $\text{In}$ ,  $\text{Cu}_7\text{In}_4$ ) with lower intensity, indicating that the solid state reaction leading to the formation of the  $\text{CuInS}_2$  films is incomplete. The presence of these minor phases is in general attributed to a sum of internal origins obeying the thermodynamics of solid solutions, to defect chemistry and the thermal gradient which plays important role as described elsewhere [16]. For  $\theta = 75^\circ$ , the peaks associated to binary compounds ( $\text{In}$ ,  $\text{Cu}_7\text{In}_4$ ) disappeared which may be related to the orientation of the polycrystalline film with persistence of the  $\text{CuInS}_2$  phase but with a decrease of the intensity of its principal peak (112). Consequently, we arrive here to eliminate the secondary phases while keeping the majority phase  $\text{CuInS}_2$ . Therefore, the thermal gradient correlates with the obliquely angle presents the advantage to get homogeneous layers for the higher incidence angles.

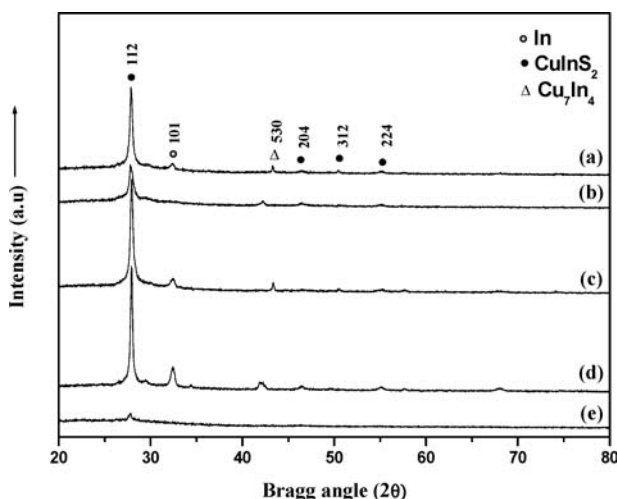


Figure 3 XRD patterns of  $\text{CuInS}_2$  films for incident angles (a)  $\theta = 0^\circ$ , (b)  $\theta = 20^\circ$ , (c)  $\theta = 40^\circ$ , (d)  $\theta = 60^\circ$  and (e)  $\theta = 75^\circ$ .

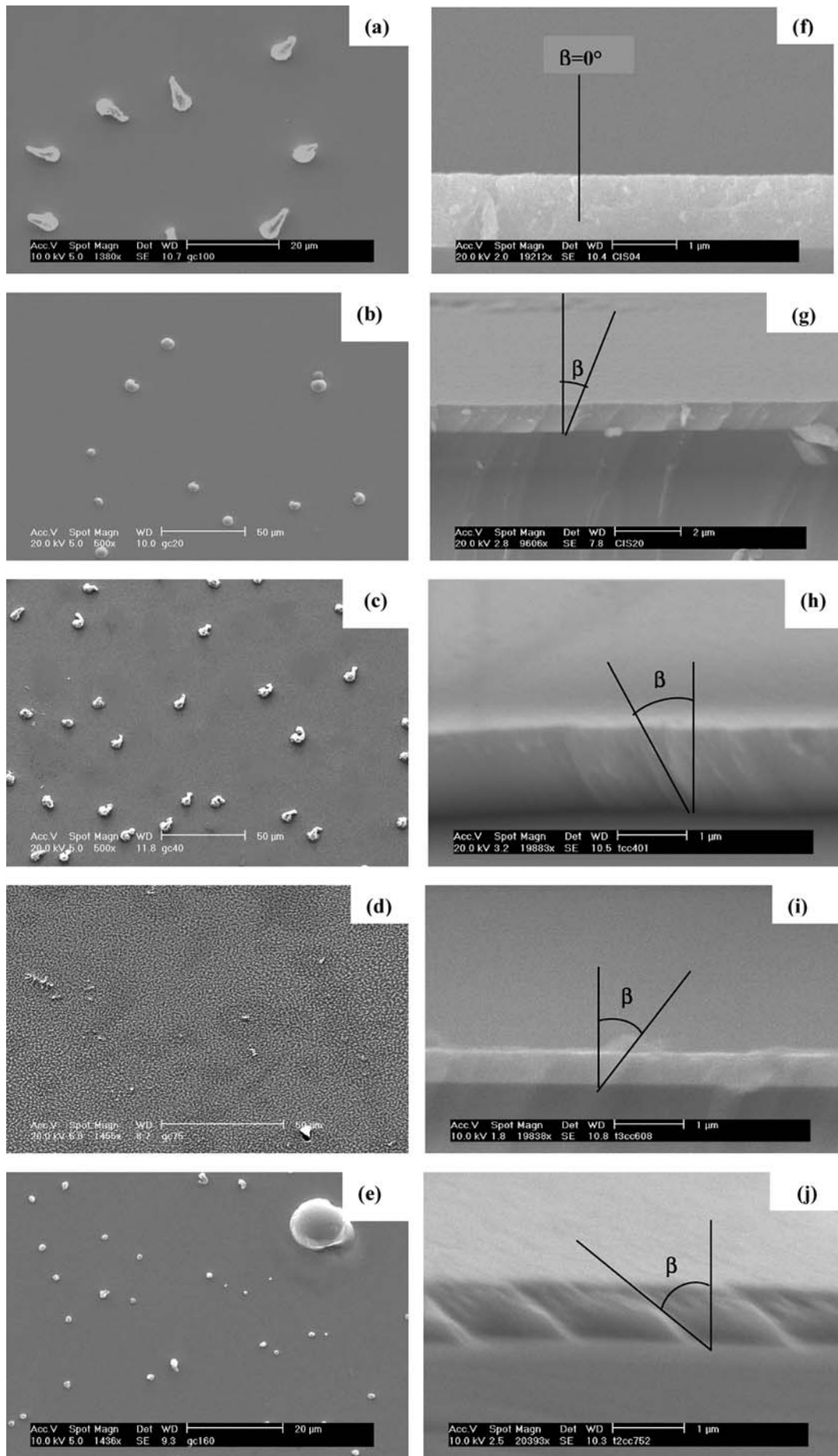


Figure 4 SEM-micrographs (surfaces and cross sections) of  $\text{CuIn}_2\text{S}_2$  films (a, f)  $\theta = 0^\circ$ , (b, g)  $\theta = 20^\circ$ , (c, h)  $\theta = 40^\circ$ , (d, i)  $\theta = 60^\circ$  and (e, j)  $\theta = 75^\circ$ .

## 3.2. Morphological properties

### 3.2.1. Surface morphology

The SEM micrographs of obliquely deposited CuInS<sub>2</sub> films confirm that the oblique angle has a great effect on the surface microstructure. Indeed, the study revealed that the film surfaces are dominated by the presence of conducting particles and an important difference in the particles distribution depending on  $\theta$  is observed. As shown in Fig. 4a–e, the particles decrease in number and in size with increasing incidence angle. Therefore, we confirm XRD results where we note a total absence of both conducting In and Cu<sub>7</sub>In<sub>4</sub> phases for the incident angle 75°.

### 3.2.2. Sectional morphology

Scanning electron microscopy (SEM) micrographs showed that thin films prepared by oblique-angle-incidence deposition had columnar microstructures that were progressively inclined as  $\theta$  was increased. Fig. 4f–j illustrate a SEM image of the cross section for films deposited at  $\theta = 0^\circ, 20^\circ, 40^\circ, 60^\circ$  and  $75^\circ$  respectively. These photographs clearly indicate that the columns grow in a preferential oblique direction, such as the tilt angle  $\beta$  is the direction of the subsequent film. In general, the column tilt angle  $\beta$  is less than the vapour incident angle  $\theta$ , and follows the empirical tangent rule,  $\tan \beta = (1/2) \tan \theta$  for small  $\theta$  ( $\theta \leq 60^\circ$ ) [12, 13], or the cosine rule,  $\beta = \theta - \arcsin(\frac{1-\cos \theta}{2})$  for higher  $\theta$  [14].

The values of  $\theta$ ,  $\beta_{\text{empirical}}$  and  $\beta_{\text{experimental}}$  are shown in the Table I given below. It has been observed that the values of  $\beta_{\text{experimental}}$  are less than that predicted from an empirical rule ( $\beta_{\text{empirical}} \approx \beta_{\text{experimental}} \pm 7^\circ$ ).

## 3.3. Optical properties

### 3.3.1. Transmission and reflection spectra

In the high absorption region (associated with interband transition) Tauc [18], and Davis and Mott [19] independently derived an expression relating the absorption coefficient  $\alpha(h\nu)$  to the photon energy ( $h\nu$ ):

$$\alpha(h\nu) = A(\alpha h\nu - E_{\text{opt}})^n / h\nu \quad (1)$$

where  $A$  is a constant ( $4\pi\sigma/nCE_c$ ),  $C$  is the speed of light and  $\sigma$  is the extrapolated d.c. conductivity at  $T = \infty$ .  $E_c$  is a measure of the extent of band tailing,  $n$  is the refractive index and  $E_{\text{opt}}$  is the optical absorption process ( $n = 1/2$  for direct allowed transition,  $n = 2$  for an indirect allowed transition,  $n = 3$  for an indirect for-

TABLE I The values of  $\theta$ ,  $\beta_{\text{empirical}}$  and  $\beta_{\text{experimental}}$

$\theta$	$\beta_{\text{empirical}}$	$\beta_{\text{experimental}}$
<i>Tangent rule</i>		
0°	0°	0°
20°	10,31°	17°
40°	22,79°	26°
60°	41°	45°
<i>Cosine rule</i>		
75°	53,24°	51°

bidden transition,  $n = 1/2$  seems to offer the best fit for the optical absorption data in chalcopyrite compound semiconductors. In the present work the absorption coefficient ( $\alpha$ ) was calculated using the relation [20]:

$$T = (1 - R)^2 \exp(-\alpha d) \quad (2)$$

where  $R$  is the reflectance,  $T$  is the transmittance,  $\alpha$  is the absorption coefficient and  $d$  is the film thickness.

For the transmission measurements, we choose the configuration for which the incident light beam falls upon the layer lengthwise [21].

Figs 5 and 6 show respectively, the transmittance  $T$  and the reflectance  $R$  spectra, for different incident angles. It is clear from the transmission spectra that high absorption films were prepared for the incident angle  $\theta$  below  $60^\circ$  ( $T\%$  is below 40% in the range 300–1800 nm). So, these high absorptions obtained at the incident angle below  $60^\circ$  could be explained by a volume effect and not by a surface effect since no changes in the reflection values have been observed in the considered spectral range.

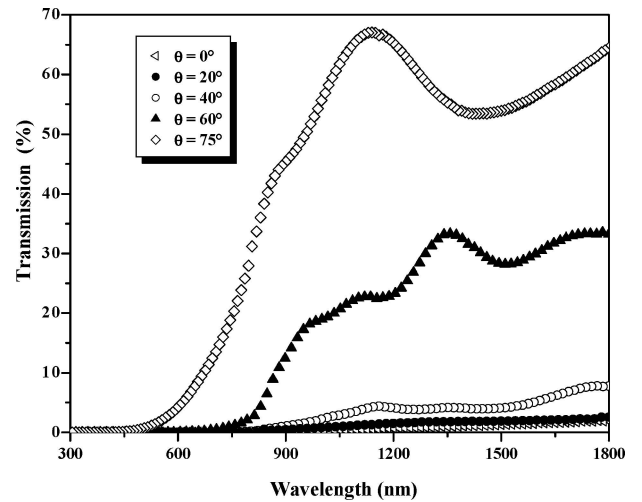


Figure 5 Transmission spectra of CuInS<sub>2</sub> films at various incident angles.

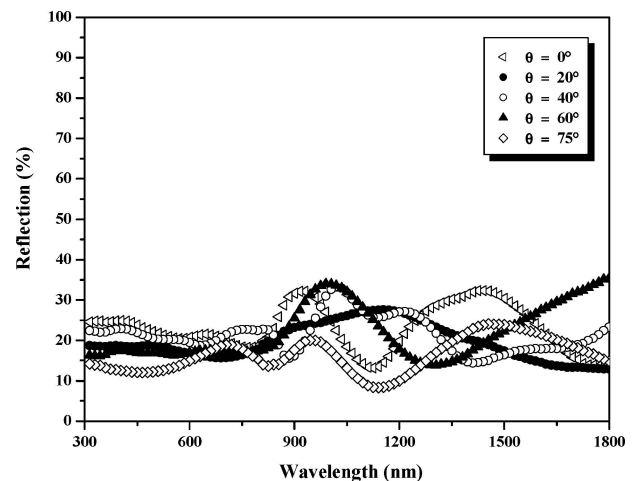


Figure 6 Reflection spectra of CuInS<sub>2</sub> films at various incident angles.

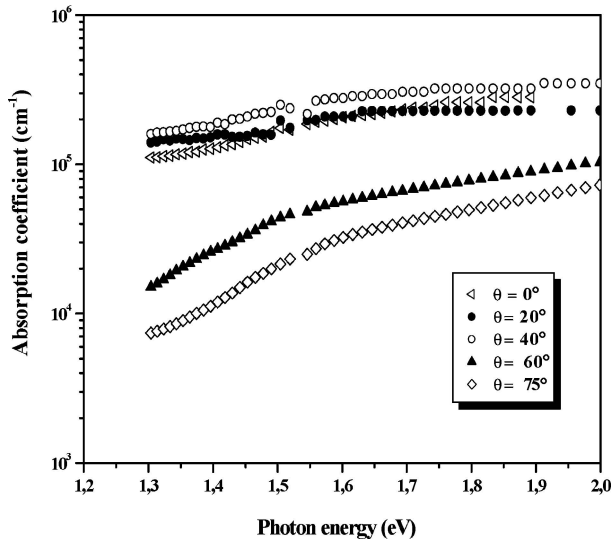


Figure 7 Absorption coefficient spectra of  $\text{CuIn}_2\text{S}_2$  films at various incident angles in presence of thermal gradient.

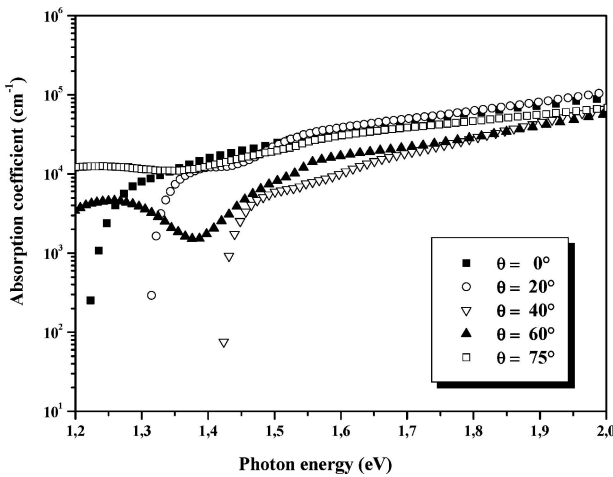


Figure 8 Absorption coefficient spectra of  $\text{CuIn}_2\text{S}_2$  films at various incident angles in absence of thermal gradient.

### 3.3.2. Absorption coefficients

The absorption coefficient  $\alpha$  was calculated for the considered incident angles (Fig. 7). It can be seen that the films deposited at the incident angle  $\theta$  below  $60^\circ$  have relatively high absorption coefficient ( $10^5$ – $3 \cdot 10^5 \text{ cm}^{-1}$ ) in the visible range and near-IR spectral range. For a comparison we show in the Fig. 8 the behaviour of the absorption coefficient for the films deposited at the incident angles  $\theta = 0^\circ, 20^\circ, 40^\circ, 60^\circ$  and  $75^\circ$  but in absence of the thermal gradient ( $d = D$ ). It is clear how the thermal gradient affects the optical properties and relatively high absorption coefficients are reached. This result is very important since the spectral dependence of the absorption coefficient affects the solar conversion efficiency [22].

## 4. Conclusion

In conclusion, we have presented experimental study of the growth of  $\text{CuIn}_2\text{S}_2$  thin films during oblique angle

deposition. It has been shown that the correlation between the obliquely angle deposition and the thermal gradient leads to an improvement in the optical properties of the films. High absorption coefficient ( $10^5$ – $3 \cdot 10^5 \text{ cm}^{-1}$ ) in the visible range and near-IR spectral range are reached for the small incident angles (i.e. close for the vapour incident angle  $\theta = 0^\circ$  with respect to the substrate normal). So, this result obtained without resorting of doping treatments is very important because we know that the spectral dependence of absorption coefficient affects the solar conversion efficiency [13].

## References

1. T. MOTOHIRO and Y. TAGA, *Appl. Opt.* **28** (1989) 2466.
2. *Idem.*, *Thin Solid Films* **185** (1990) 137.
3. K. KUWAHARA and S. SHINZATO, *ibid.* **164** (1988) 165.
4. M. MICHIJIMA, H. HAYACHI, M. KYOHO, T. NAKABAYASHI, T. KOMODA and T. KIRA, *IEEE Trans. on Magn.*, **35**(5) (1999).
5. H. EL. SHAIR, M. M. EL-NAHASS, A. M. IBRAHIM, H. S. SOLIMAN, N. M. KHALIL, B. A. KHALIFA and A. A. EL-SHAZLY, *J. Mater. Sci. Lett.* **9** (1990) 540.
6. V. N. VIGDOROVICH, G. A. UKHLINOV, F. CH. KARIMOV and D. M. KRASNOV, *Izv. Akad.Nauk SSSR Neorg. Mater.* **23** (1987) 1081.
7. HO HUEI-MIN, G. J.-S. GAU and G. THOMAS, *J. Appl. Phys.* **65** (1989) 3161.
8. K. OKAMOTO, K. ITOH and T. HASHIMOTO, *J. Magn. Magn. Mater.* **87** (1990) 379.
9. J. M. ALAMEDA, F. CARMONA, F. H. SALAS, L. M. ALVAREZ-PRADO, R. MORALES and G. T. PEREZ, *ibid.* **154** (1996) 249.
10. S. HAMZAOU, M. LABRUNE, I. B. PUCHALSKA and C. SELLA, *J. Magn. Magn. Mater.* **22** (1980) 69.
11. A. LISFI and J. C. LODDER, *Phys. Rev. B* **63** (2001) 174441.
12. J. M. NIEUWENHUIZEN and H. B. HAANSTRA, *Philips Tech. Rev.* **27** (1966) 87.
13. A. G. DIRKS and H. J. LEAMY, *Thin Solid Films* **47** (1977) 219.
14. R. N. TRAIT, T. SMY and M. J. BRETT, *ibid.* **226** (1993) 196.
15. J. KLAER, J. BRUNS, R. HENNINGER, K. SIEMER, R. KLENK, KELLMER and D. BRÄUNIG, *Semicond. Sci. Technol.* **13** (1998) 1456.
16. M. KANZARI, M. ABAAB, B. REZIG and M. BRUNEL, *Mater. Res. Bull.* **32** (1997) 1009.
17. K. L. CHOPRA, "Thin Film Phenomena" (McGraw-Hill, New York, 1969) p. 721.
18. J. TAUC, in *Optical Properties of Solids*, edited by F. Abeles (North Holland, Amsterdam, 1970) p. 903.
19. E. A. DAVIS and N. F. MOTT, *Phil. Mag.* **22** (1970) 903.
20. T. S. MOSS, *Optical Properties of Semiconductors*, Butterworth, London, 1959.
21. M. KANZARI, M. ABAAB, K. S. ABDELKARIM and B. REZIG, *16th European Photovoltaic Solar Energy Conference*, 1–5 May 2000, Glasgow, UK.
22. V. V. KINDYAK, V. F. GREMENONOK, I. V. BODNAR, V. RUD YU and G. A. MADVEDKIN, *Thin Solid Films* **250** (1994) 33.

Received 18 November 2004  
and accepted 23 March 2005